PERFORMANCE MODELS FOR AN EMULSION-TREATED MATERIAL UNDER ACCELERATED PAVEMENT TESTING[*]

J J E LIEBENBERG[1] and A T VISSER[2]

[1]Stewart Scott (Pty) Ltd, P O Box 784506, Sandton, 2146
[2] Department of Civil Engineering, University of Pretoria, Pretoria, 0002

1. INTRODUCTION

During the last 30 years, South African engineers have achieve great success in adding small quantities of bitumen emulsion to gravels of marginal to good quality to provide materials that could cater for the highest pavement design categories. Since the introduction of deep in-situ recycling (DISR) into South Africa, the use of bituminous emulsion and foam bitumen in base layers has become more attractive and the extent of use has been greatly increased. The ageing road network in South Africa, as well as increasing demands in minimum disruption to road users during road construction and rehabilitation, required innovative measures that do not sacrifice the structural integrity of the rehabilitated or newly constructed pavement. The advantages associated with the use of bitumen emulsion include:

- The ability to open rehabilitated roads to traffic shortly after construction, thereby eliminating the construction of expensive detours and minimising disruption to road users.
- Cheaper construction costs than most standard methods of rehabilitation (World Highways: 2001)
- Marginal materials can be utilised in pavement layers

Although emulsion-treated materials have been used with great success for a number of years, their structural performance has not been investigated in detail. Research is currently under way to assess their use in the road building industry. The research includes the use of the Heavy Vehicle Simulator (HVS), laboratory testing and field trials. Results from this research will create a knowledge base on the structural design from which guideline documents and design methods can be developed. The major aspects that are being investigated include:

- The engineering properties such as bearing strength, permeability and erodibility.
- The mechanical properties such as stiffness, shear strength and strain at break.
- The behaviour of the material and pavement under repeated loading.
- Aspects that impact on the above such as design, construction and maintenance.

This paper discusses the results from HVS and laboratory testing on an emulsion-treated material. The HVS test results were used to determine structural design and performance models for fatigue and permanent deformation for the materials tested. These models were then used to estimate load sensitivity and damage factors.

---

[*] This paper is based on research carried out by the first author towards a MEng degree at the University of Pretoria

2. TEST SECTION MATERIALS AND CONSTRUCTION

The HVS test sections were constructed on road P 243/1 between Vereeniging and Balfour in the Gauteng province of South Africa. The original pavement structure before rehabilitation consisted of an asphalt surfacing, cement stabilised ferricrete base layer and untreated ferricrete subbase layer. The rehabilitation design of the pavement consisted of a 25 mm asphalt surfacing and 250 mm deep in-situ recycled layer stabilised with 2% cement and 3% bitumen emulsion (1.8 % net bitumen). The lower layers were left intact. The recycled layer contains the milled surfacing and ferricrete from the original base and subbase layers. The main properties of the material are presented in Table 1. The gradation of the material is shown in Figure 1 and is similar to that of a crushed stone material (Long and Theyse: 2001). The material has a G7 classification according to TRH14 (CSRA: 1987)

Table 1. Engineering properties of milled ferricrete

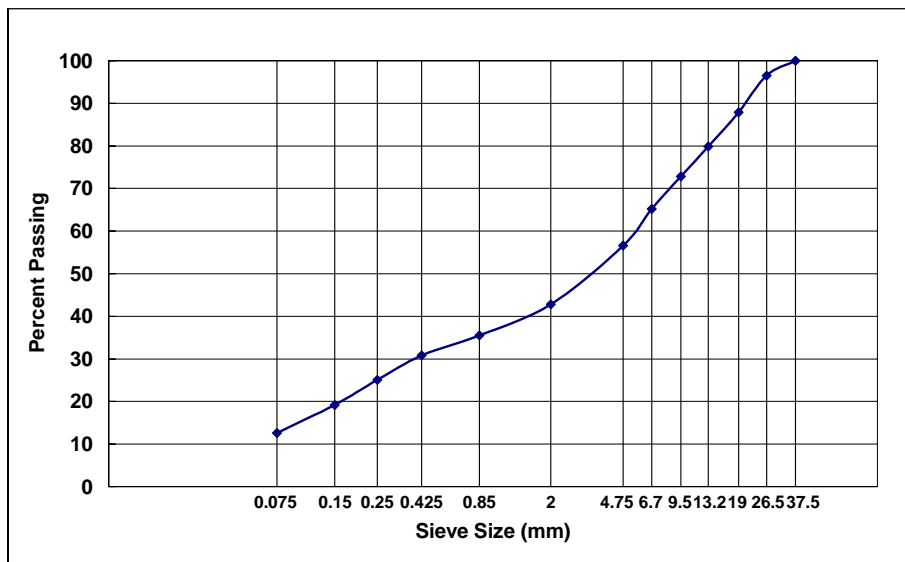| Property	Value
Maximum dry density (MDD)	1 971 kg/m3
Optimum moisture content (OMC)	12.5 %
Grading modulus (GM)	2.13
Plasticity index (PI)	7
CBR @ 93%	18
CBR @ 98%	56

Figure 1. Grading of milled untreated ferricrete material

3. LABORATORY TESTING

3.1 Laboratory tests and results

A number of laboratory tests were conducted on the material with various cement and emulsion contents. The testing included California Bearing Ratio (CBR), Indirect Tensile Strength (ITS), Unconfined Compressive Strength (UCS), flexural beam tests and static and dynamic triaxial tests. The CBR, UCS and ITS tests are not discussed in this paper. These results are discussed by Long and Theyse (2001) and Liebenberg (2001).

3.2 Flexibility

The flexibility of the treated materials were determined with the four point static beam test. The strain at break value is interpreted as the strain at which microcracks will start to initiate. The results are shown in Figure 2 for various cement and net bitumen contents.
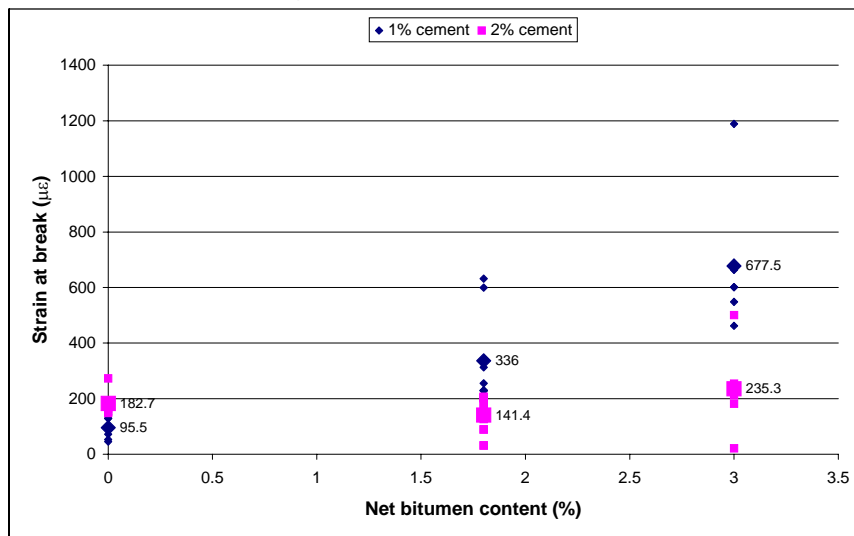

Figure 2. Strain at break values for various cement and net bitumen contents

Generally the strain at break increases with an increase in net bitumen content. At lower net bitumen contents the strain at break is similar to that of lightly cemented materials. An increase in the cement content resulted in a decrease in the strain at break. The flexibility of the material therefore increased with an increase in binder content, but decreased with an increase in cement content.

3.3 Shear strength

The static shear strength of the material was determined by static triaxial tests. A summary of the results from the static triaxial tests is presented in Table 2.

For the cement treated material the cohesion and friction angle is insensitive to the degree of saturation. The shear strength is therefore more dependent on the chemical bonding from the cement than on the suction generated by negative pore pressures. For the emulsion-treated material it appears that the cohesion and friction angle tend to influence each other. Due to this model effect the indirect method as described by Lambe et al (1996) and Das (1990) were used to determine the shear strength parameters. This method uses a method where *p and q* are plotted against each other from where the shear stress parameters can be calculated. The parameters *p* and *q* are calculated as follows:

$$p = \frac{\sigma_1 + \sigma_3}{2} \qquad \text{and} \qquad q = \frac{\sigma_1 - \sigma_3}{2}$$

with σ_1 and σ_3 the major- and minor principal stresses respectively. The parameter p gives an indication of the axial stress while q an indication is of the shear stress.

The cohesion and friction angle calculated by the indirect method were 308 kPa and 50.9° respectively for all the saturation and relative densities within the stress conditions tested. The relative density is the percentage density relative to the apparent density of the material.

Table 2. Static triaxial test results calculated directly from Möhr circles
(Long and Theyse: 2001)

Cement content (%)	Net bitumen content (%)	Relative Density (%)	Saturation (%)	Cohesion (kPa)	Friction angle (degrees)
0	0	86	79	20	43.1
0	0	86	56	37	39.7
0	0	96	79	31	41.0
0	0	96	56	126	40.1
2	0	70	73	333	50.9
2	0	70	63	337	50.5
2	1.8	70	64	543	32.5
2	1.8	70	59	329	46.5
2	1.8	73	64	458	48.3
2	1.8	73	59	370	54.8

3.4 Laboratory elastic modulus

The dynamic triaxial test results were used to calculate the elastic or resilient stiffness of the material. The dynamic triaxial tests were performed at two densities and saturation levels and three stress ratios. The stress ratio of a material is the ratio between the applied stress and the maximum shear strength at the failure envelope of the material.

The elastic modulus of material ranged between 1 200 MPa and 2 700 MPa with an average of 2 039 MPa and a standard deviation of 450 MPa. Figure 3 presents the influence of the different test parameters on the resilient modulus.
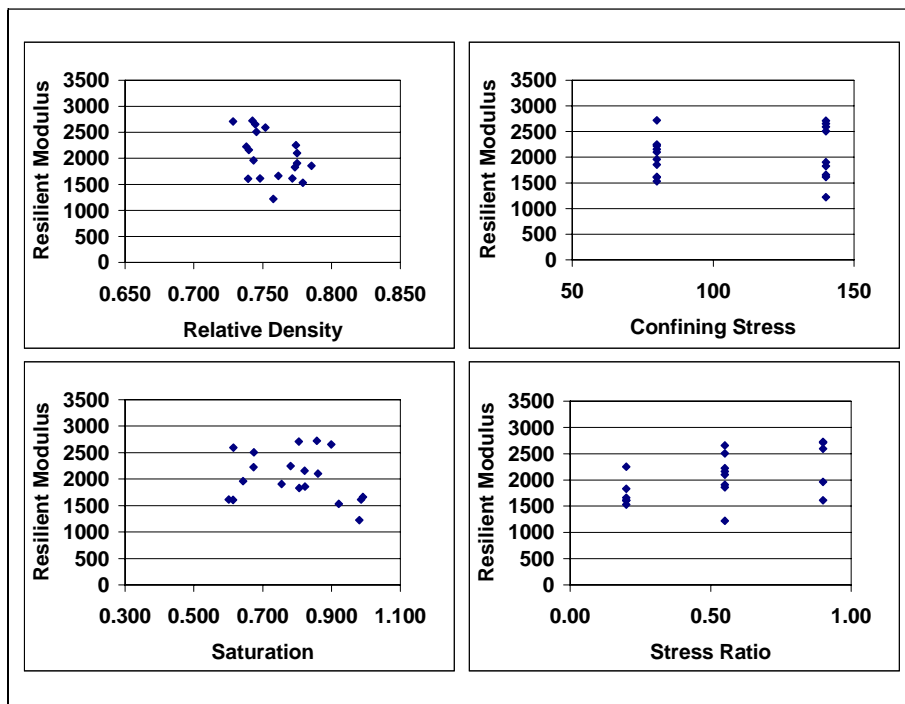

Figure 3. Resilient modulus as a function of the various laboratory test variables

3.5 Permanent deformation

A major objective of the laboratory testing was to develop design models from the laboratory test results that could be compared to the permanent deformation behaviour of the materials under HVS testing. A model in the form of Equation (1) (Theyse: 2000), that describes the permanent deformation behaviour of materials, was fitted to all the reasonable data from each dynamic triaxial test. For the data fitted, the model fits were reasonable.

$$PD = mN + \frac{cN}{\left[1 + \left(\frac{cN}{a}\right)^b\right]^{\frac{1}{b}}} \qquad (1)$$

where: PD = Permanent deformation (mm)
N = number of load repetitions
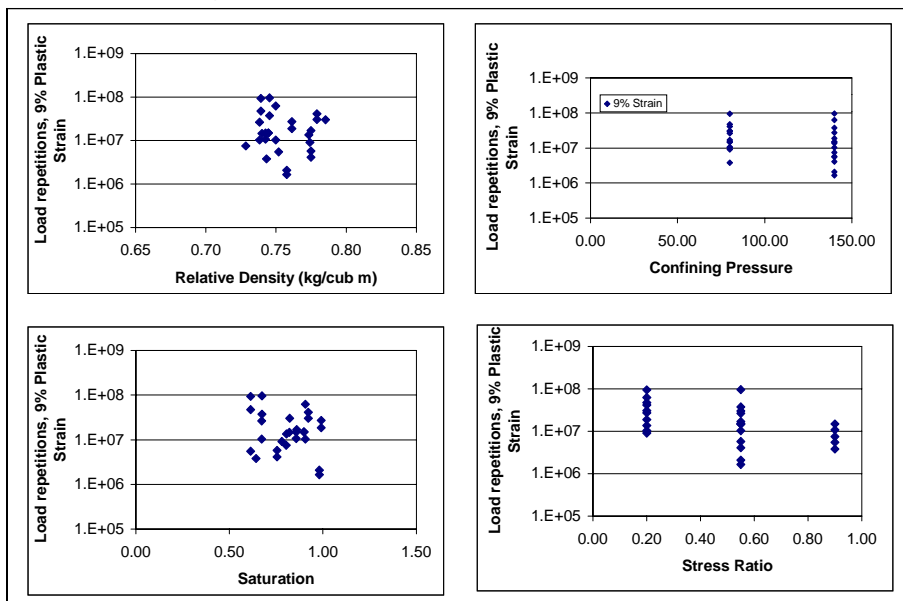a, b, c, m = regression coefficients

Figure 4. The influence of relative density, degree of saturation and stress ratio on the number of load repetitions to 9 % plastic strain

The number of load repetitions for permanent deformation is largely insensitive to the relative density and degree of saturation when the sample is treated with bitumen emulsion. The results for an untreated ferricrete, as documented by Long and Theyse (2001), showed sensitivity towards relative density and saturation for untreated samples. The stress ratio however seems to have some influence on the number of load repetitions to 9 % plastic strain, although a high amount of scatter is present. From the results published by Long and Theyse (2001), there was no significance in the improvement of the permanent deformation resistance by the addition of bitumen emulsion compared to the untreated and cement only treated samples as tested under dynamic triaxial tests.

4. HEAVY VEHICLE SIMULATOR TESTING

Basically three test sections were tested under the HVS. Sections 410A4 and 410B4 overlapped 4 m, while section 412A4 was a completely separate section. The location of the test sections was selected from areas of fairly uniform falling weight deflectometer deflections. The initial analyses of the test sections were described by Steyn (2001) and Mancotywa (2001).

4.1 Test programme and instrumentation

Three test sections were tested at 80, 100 and 40 kN wheel loads. The 100 kN test section overlapped 4 m with the 80 kN test. The tyre pressures were varied to ensure a uniform load contact area on the test section. Table 3 provides a summary of the test conditions on the test sections.

Table 3. Summary of HVS testing on sections 410A4, 410B4 and 412A4

Section	Dry/wet	Load applications	Trafficking load (kN)	Tyre inflation pressure (kPa)
410A4	Dry	295 617	80	800
410B4	Dry	171 500	100	850
	Wet	13 907	80	800
412A4	Dry	957 121	40	620
	Dry	App 350 000	80	800
	Wet	App 50 000	80	800

All three the tests were done under nominally dry conditions and no testing was allowed during rain. The load was applied at a speed of 8 km/h using a wandering pattern of 1 m wide. The wandering pattern was obtained by allowing the test beam to move 50 mm sideways on a side after each load application. This process caused the wandering pattern to simulate a normal distribution of load applications on the test section as would be expected from normal traffic (Blabb and Litzka: 1995). The tyre pressures were adjusted to ensure a uniform contact area between the tyre and the pavement during the testing (Steyn: 2001).

The standard HVS instruments were used to evaluate the performance of the test section under HVS testing. These included the Straight edge, Laser Profilometer, Road Surface Deflectometer (RSD), Multi Depth Deflectometer (MDD) and Thermocouples

Cracks on the surface were monitored and photographed at regular intervals during the test cycle.

4.2 Permanent deformation

Permanent deformation measured by the Laser Profilometer indicated low values on all the sections during the dry phase of the tests. The permanent deformation on the surface was less than 2 mm before water was added to the pavement where after it increased to between 5 and 6 mm.

The pavement in depth deformation, measured by the MDD, on all the sections was also reasonably low with values of between 1 and 3 mm permanent surface deformation during the dry phase of the tests. The MDD measurements indicated that most of the permanent deformation occurred in the treated base layer (20 – 275 mm).

Table 4 presents a summary of the permanent deformation data modelled for each of the measuring devices for each test section. The permanent deformation measurements that were measured by the different devices were very small, and factors like texture depth and human error (on the straight edge), could have a significant influence. The data from the MDD's were mainly used in the analysis and development of a structural design model.

Table 4 Summary of permanent deformation results from HVS tests

Section	Load (kN)	Expected rut after 1 million loads (mm)					Expected Load repetitions to 20 mm rut (millions)				
		LP	SE	MDD 4	MDD 8	MDD 12	LP	SE	MDD 4	MDD 8	MDD 12
410A4[*]	80	11.1	2.2	8.9	-	7.8	1.80	9.09	1.12	-	1.28
Overlap[*]	80/100	3.3	10.2	-	-	-	6.06	1.96	-	-	-
410B4[*]		9.1	10.7	17	-	32	2.20	1.87	0.59	-	0.31
412A4	40	2.0	0.7	1.3	1.8	0.4	24.8	71.5	61.2	33.2	50.7

[*]After Steyn (2001)   LP = Laser profilometer

Note: MDD module at 20 mm depth   SE = Straight edge

4.3 Elastic deflections

The elastic deflections were measured at various points on the surface by the Road Surface Deflectometer (RSD) and in depth by MDD's. The maximum elastic deflections for the three test sections are presented in Figure 8.
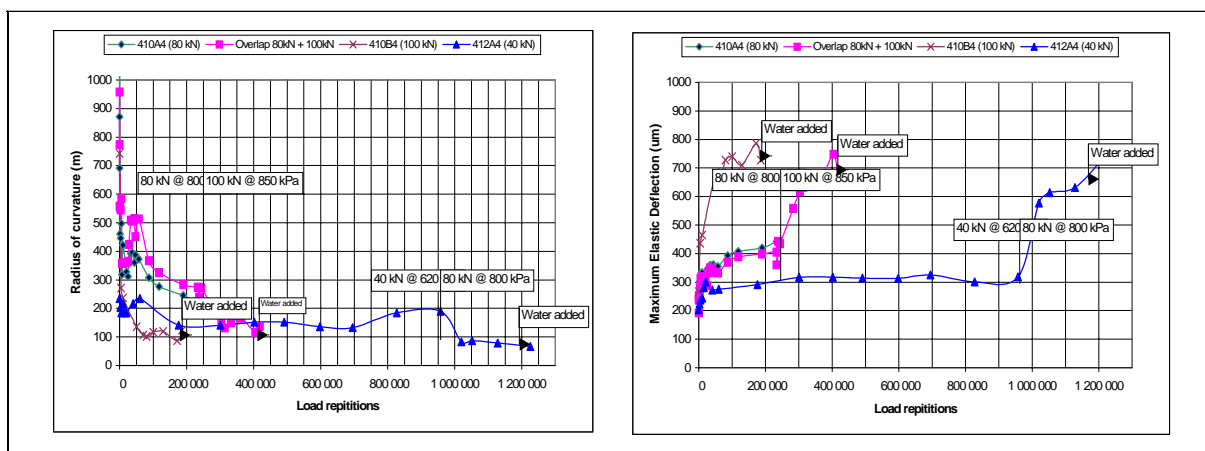

Figure 5. Maximum elastic deflection and Radius of curvature

The deflection bowls from the RSD data indicate the influence of an increasing wheel load on the maximum deflection and shape of the deflection bowl. The radius of curvature decreases while the maximum deflection increases with an increase in wheel load. The most obvious influence is however on the maximum deflection. The radius of curvature (*ROC*) showed that there is a change in the elastic behaviour of the pavement structure during trafficking. The structure loses its bearing capacity in the upper layers and starts to transfer the load deeper into the structure. This change in elastic behaviour is not as distinct as in the case with cement treated layers (de Beer: 1989), and it seems that layers treated with emulsion change their elastic behaviour more gradually during trafficking. The *ROC* also decreases when the trafficking wheel load is increased which indicates that the pavement structure tends to reduce its load spreading capability in the upper layers.

4.4 Backcalculated elastic stiffness

The depth deflection profiles were used to back-calculate the effective elastic moduli (E – moduli) for the different layers at various stages of trafficking. The subgrade was assumed to be of infinite depth i.e. an elastic half space with a stiff layer at a depth of approximately 2.5 m. A Poisson's ratio of 0.35 was used in the backcalculation and an analysis at different Poisson's ratios indicated that the stiffnesses were not sensitive to changes in Poisson's ratio values.

The results show that the E - moduli decrease gradually with trafficking. For higher wheel loads this reduction is more rapid than for lower wheel loads. It is believed that this reduction in E moduli, together with the change in the shape of the deflection bowl will enhance the understanding of the behaviour of emulsion-treated layers in terms of fatigue and permanent deformation.

Table 5 and Figure 6 present the backcalculated E moduli for the three test sections at the beginning and end of each test.

Table 5 Summary of backcalculated E moduli for HVS test sections.

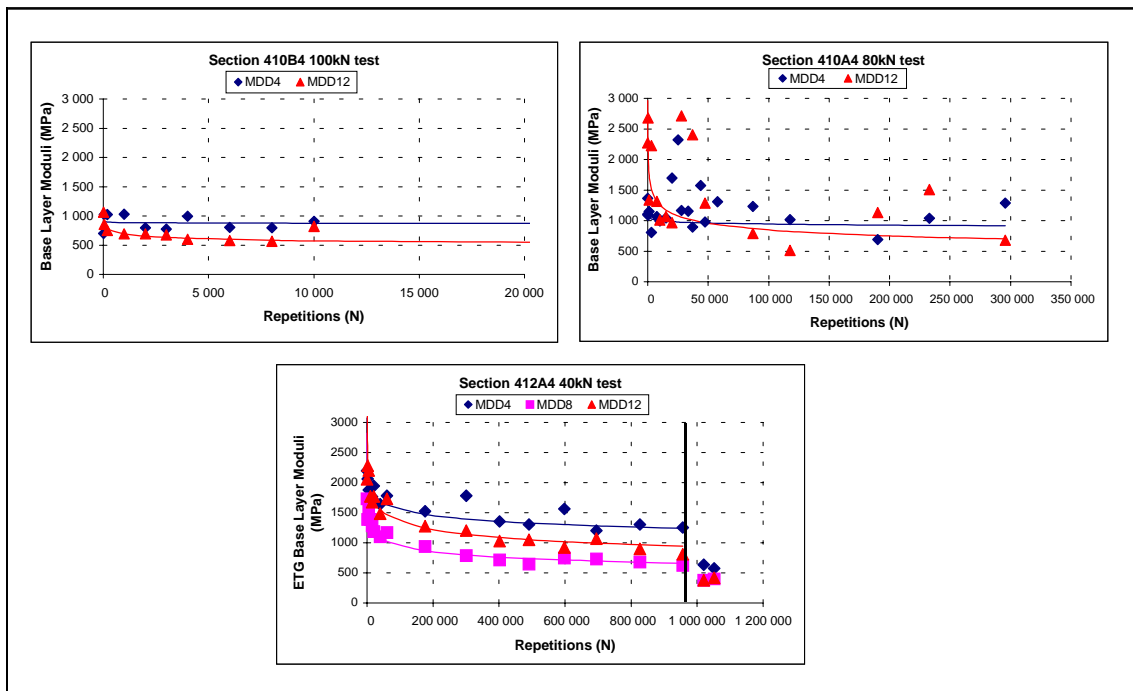| Section	Trafficking load	Initial Stiffness (MPa)	Stiffness at end (MPa)	Number of repetitions
410A4	80 kN	2 000 – 2 700	1 100	295 617
Overlap	80 kN	2 000 – 2 700	1 000	295 617
	100 kN	1 000	850	467 117
410B4	100 kN	1 000	750	171 500
412A4	40 kN	1 750 – 2 250	750 – 1 250	957 121
	80 kN		350 – 500	1 321 700

Figure 6 Backcalculated E-moduli for the different test sections

All the tests started at an initial effective E - modulus of between 1 750 and 2 700 MPa that agrees well with the dynamic triaxial test results from the laboratory tests. A rapid reduction in the E moduli early after trafficking started on all the sections followed by a more gradual decrease in stiffness with increase in load repetitions. The terminal stiffness, when the material broke down to some post-cracked or fractured state seems to converge to a value in the order of 500 MPa which agree well with values from dynamic triaxial tests on the recycled, untreated ferricrete (Long and Theyse: 2001).

4.5 Crack development

Surface crack development was monitored visually. Surface cracking only initiated late in the tests as presented in Table 6. This could be as a result of the fresh asphalt surfacing layer over the emulsion-treated base layer.

Table 6 Crack development on HVS test sections

Test section	Number of repetitions before surface cracking was detected
410A4	No cracking developed before test was terminated at 295 617 reps.
410B4	129 544
412A4	1 321 700[*]

[*] First 957 121 repetitions were at 40 kN and the last 364 579 at 80 kN

4.6 Visual observations and test pits

The layer broke down into large lumps during the 80 and 100 kN tests (sections 410A4 an 410B4) but during a visual inspection no indication of this could be found after the 40 kN test (section 412A4).

On the 40 kN test, no cracks in the emulsion-treated layer could be observed throughout the depth profile of the test pit. The cracks that reflected on the surface of the road were only in the asphalt layer and none of these cracks could be followed into the emulsion-treated layer. Since most of the cracking only started during the wet part of the tests, the cracks in the asphalt surfacing were the result of higher deflections (greater than 1 000 μm) in the underlying layers under trafficking in the wet conditions. The asphalt layer therefore failed in fatigue.

Some of the finer material from the emulsion-treated layer migrated towards the sides of the test section during the wet phase of the tests. Since no cracking was present the fines were displaced sideways rather than pumped out through the cracks.

4.7 Discussion

The emulsion-treated test sections performed well during the HVS tests. The thickness of the treated recycled layer (250 mm) could have contributed to this performance of the pavement. Little permanent deformation was measured at the surface throughout the dry phases of the tests with crack development mainly restricted to the wet tests. Although most of the permanent deformation occurred within the emulsion-treated layer, the amount of permanent deformation was negligible. The small contribution of the lower layers to the permanent deformation as well as the elastic deflection, indicate that the emulsion-treated layer provided good protection for the subgrade and other lower lying layers.

The reduction in the E - moduli and gradual change in the deflection bowl, confirm that the behaviour of emulsion-treated layers is a phased behaviour. The material initially has a high elastic modulus with low deflections. Most of the load is being spread in the base layer (large radius of curvature). As the material moves into a second phase, the modulus of elasticity reduces and more of the load is being transferred deeper into the pavement. This resulted in higher deflections from the lower layers and a smaller radius of curvature. The test pits revealed that the second phase might not necessarily be a so called "equivalent granular" phase, but rather a phase with a reduced stiffness in which the permanent deformation of the layer (as a base layer) may be the dominant failure mechanism. The mechanism of the permanent deformation could be similar to that present in unbound granular base layers, which is a combination of gradual shear failure and densification or compaction during the initial bedding in phase (Wolff: 1992 and Theyse: 2000).

5. STRUCTURAL DESIGN AND PERFORMANCE MODELS

From the HVS and laboratory data it is possible to determine preliminary structural design and performance models for use in mechanistic-empirical pavement design. At the time of writing this paper, the final HVS tests had just ended and the development of permanent deformation models are being still researched. The final version of this paper will include those models.

The two major forms of distress on the HVS test sections were fatigue and permanent deformation.

5.1 Fatigue

The backcalculated stiffnesses from the in-depth MDD data were used to determine a structural design model for fatigue. During the post-cracked phase the material started to develop microcracks at the bottom of the layer. The cracks then progressed through the layer, reducing the stiffness of the layer to that equal to a granular material. This is known as the effective fatigue life. The effective fatigue life was defined as the life where the stiffness of the material converges to a value of around 500 MPa for this particular ferricrete. A transfer function for the effective fatigue life is described in Equation (2) and presented in Figure 7.

$$N_{eff} = 10^{6.344\left(1 - \frac{\varepsilon_t}{7.4\varepsilon_b}\right)} \qquad (2)$$

where: N_{eff} = Effective fatigue life

ε_t = calculated tensile strain at the bottom of the layer

ε_b = strain at break

The slope of the line is similar to that of lightly cemented materials as determined by de Beer (1989). The behaviour of emulsion-treated materials is similar to that of a cement treated material but with an increase in flexibility.
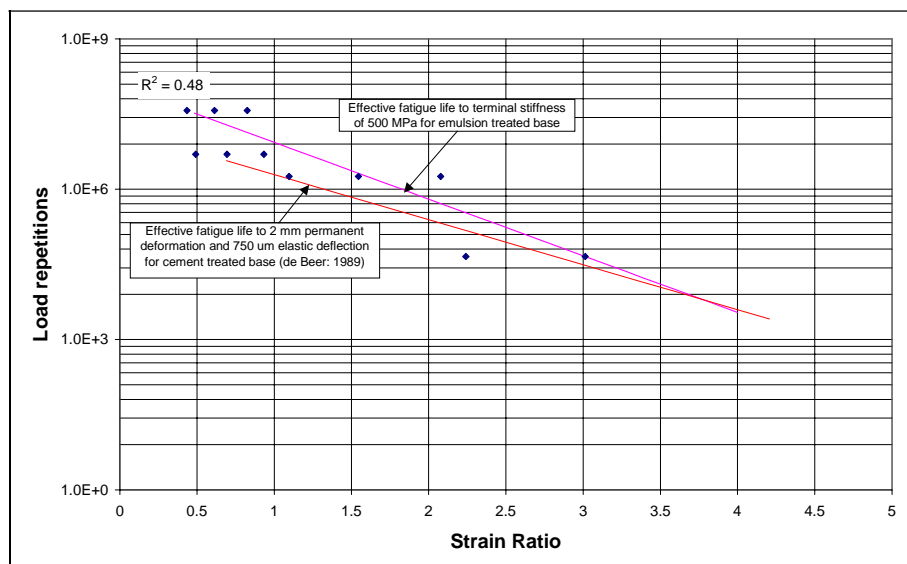

Figure 7 Effective fatigue life of an emulsion-treated ferricrete

5.2 Permanent deformation

Structural design models for permanent deformation were developed from the in-depth permanent deformation measured by the MDD's.

The data from the MDD's were used to fit a regression model in the form of Equation (3). The justification of this model is discussed by Theyse (2000).

$$PD = mN + a\left(1 - e^{-bN}\right)$$ (3)

where: PD = Permanent deformation

N = number of load repetitions

m, a, b = regression coefficients

Because of the variation in the MDD data along a test section, the model was fitted to each MDD from all the tests, rather than averaging the data. The permanent deformation for the base layer was determined by the difference in the permanent deformation between the top MDD module and the one at the bottom of the base layer (250 mm).

The model fits were used to determine a simple model to predict the number of load repetitions to a certain level of permanent deformation or plastic strain. The model is formulated in terms of plastic strain (permanent deformation divided by initial layer thickness) to account for the layer thickness. The model in terms of Stress Ratio is presented in Figure 8. The Stress Ratio is defined by Equation 4 and the development thereof is described in detail by Theyse (200). The model assumes that the pavement structure be analysed using multi-layer linear elastic theory (Theyse: 1996).

The calculated critical Stress Ratio in the layer varies with depth and relative to the position of the loads. The recommended positions of the critical stress ratios are indicated in Figure 8. The critical Stress Ratio in the layer was calculated to determine the transfer function for permanent deformation and the transfer function for different degrees of plastic strain is presented in Figure 9 and Equation 5.
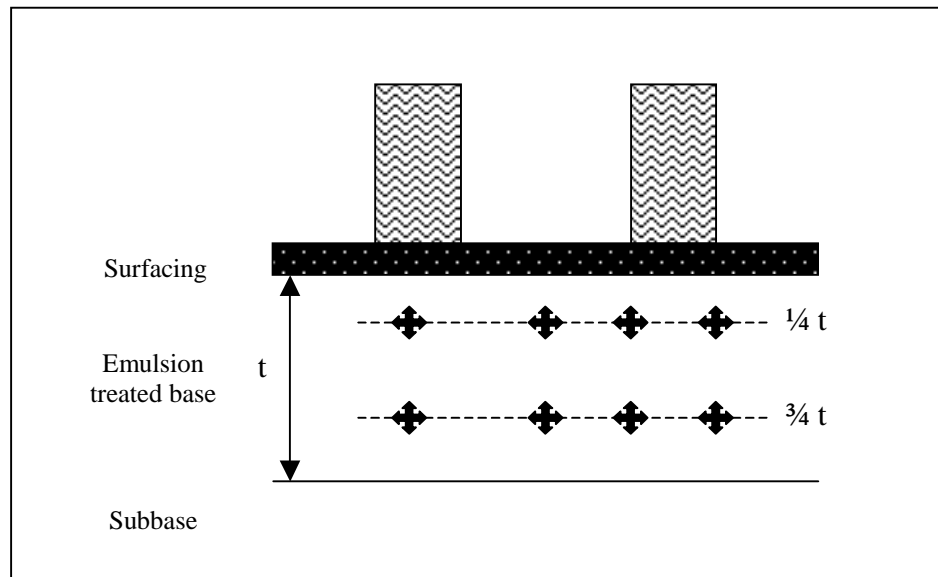

Figure 8. Recommended positions to calculate the critical Stress Ratio

$$SR = \frac{\sigma_1^a - \sigma_3^a}{\sigma_1^m - \sigma_3^a} = \frac{\sigma_1^a - \sigma_3^a}{\sigma_3^a \left(\tan^2\left(45 + \frac{\phi}{2}\right) - 1\right) + 2.c\tan\left(45 + \frac{\phi}{2}\right)}$$ (4)

where: SR = Stress Ratio
σ_1^a = Applied major principal stress
σ_1^m = Maximum allowable major principal stress
σ_3^a = Applied minor principal stress
c = cohesion (kPa)
ϕ = Friction angle (degrees)
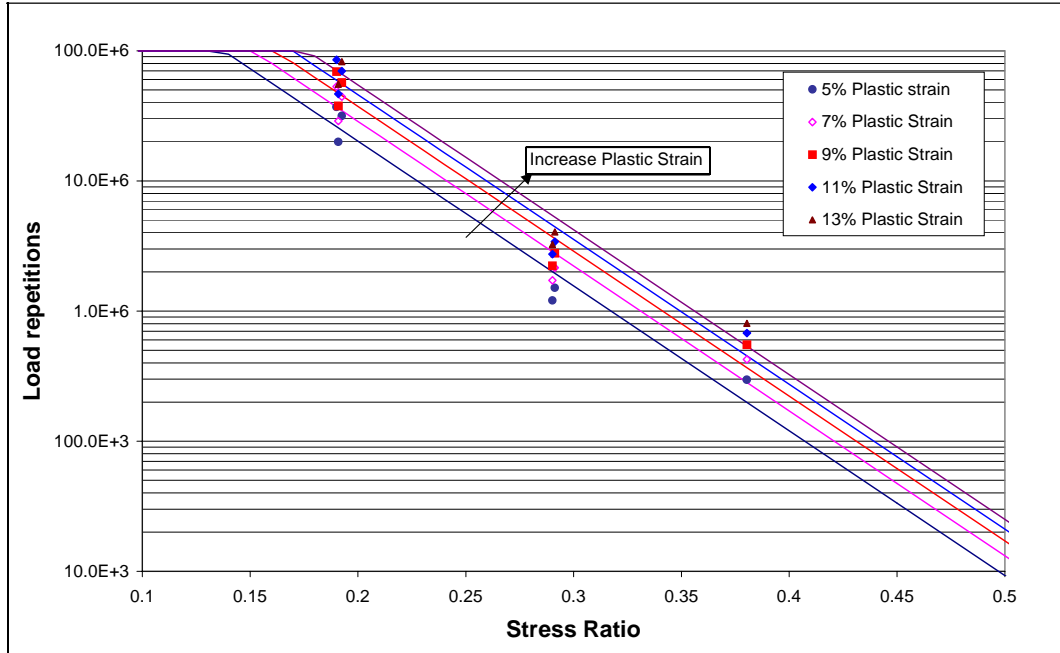

Figure 9. Permanent deformation model for emulsion treated ferricrete

$$N = 10^{9.298165 + \frac{PD}{18.78} - \frac{13.13}{SR}}$$ (5)

where: N = Number of load applications to % permanent deformation

PD = % Permanent deformation

SR = Critical Stress Ratio

5.3 Load sensitivity and Damage Factor

The HVS data can also be used to determine the load sensitivity and damage factors for the material. The damage factor, n, is used in Equation 6 to determine the damage caused by a particular wheel load relative to the damage caused by a standard wheel load.

$$\left(\frac{N_x}{N_{std}} \right) = \left(\frac{P_x}{P_{std}} \right)^n$$ (6)

where: N_x = load repetitions at wheel load
N_{std} = load repetitions at standard wheel load
P_x = wheel load
P_{std} = standard wheel load
n = damage factor

Damage factors were calculated by relating a certain defect under a 80 kN and 100 kN wheel loads to that defect under a 40 kN wheel load. The 40 kN HVS wheel load is equivalent to a 80 kN standard axle load.

Damage factors were calculated for permanent deformation as well as fatigue. The damage factors are presented in Table 8.

The high variation in the fatigue damage factor is the result of the difference in the fatigue behaviour between the different MDD's at a test section. The value published here could be used as an interim guideline until further research develops definitive values.

Table 8. Damage factors for emulsion-treated gravel

| | | 40 kN wheel load (section 412A4) | | |
		MDD4	MDD8	MDD12
		Permanent Deformation		
80 kN wheel load (section 410A4)	MDD4	5.77	4.89	5.50
	MDD12	5.58	4.70	5.31
100 kN wheel load (section 410B4)	MDD4	5.07	4.40	4.86
	MDD12	4.22	3.55	4.02
	Average		*4.82*	
	Std deviation		*0.68*	
		Fatigue		
80 kN wheel load (section 410A4)	MDD4	10.70	1.50	4.36
100 kN wheel load (section 410B4)	MDD4	8.16	1.11	3.31
	Average		*4.87*	
	Std Deviation		*3.85*	

6. CONCLUSIONS

This paper presented the data and analyses from accelerated pavement testing by the HVS on an emulsion-treated material recycled with a deep in-situ recycler. The HVS test sections performed well in the dry condition and most distress only started to develop after water was added during trafficking. The elastic deflection data were used to backcalculate the effective elastic stiffnesses and these data showed that the stiffness of the treated material rapidly decreases initially, with a more gradual decrease towards an 'equivalent granular state'. The 'equivalent granular state' was reached, regardless of the load, when the stiffness converged towards a value of around 500 MPa that was the stiffness of the virgin ferricrete material.

The laboratory tests indicated that the addition of cement strengthens the material while the emulsion contributes to the flexibility. A fine balance is therefore necessary to ensure the optimum combination of these stabilisers.

From the structural design models, damage factors were estimated for fatigue and permanent deformation. The damage factor for both types of distress were in the order of 4.85, although further research is necessary to confirm the fatigue damage factor.

Structural design models developed from the HVS test data could be used in similar conditions than the conditions tested. This includes deep in-situ recycling of natural gravel materials, but the models were not developed for, and might not be applicable to emulsion-treated crushed stone materials.

7. ACKNOWLEDGEMENTS

8. REFERENCES

Committee of State Road Authorities (CSRA), 1987, *Guidelines for Road Construction Materials*, TRH14: 1987, Department of Transport, Pretoria.

Das BM, 1990, *Principles of Geotechnical Engineering*, 2nd ed., PWS-KENT Publishing Company, Boston.

De Beer M, 1989, *Aspects of the design and behaviour of road structures incorporating lightly cementitious layers*, PhD thesis, University of Pretoria, Pretoria.

Lambe FM and Whitman RV, 1969, *Soil mechanics*, Massachusetts Institute of Technology, John Wiley & Sons Inc., New York.

Liebenberg JJE, 2001, *The influence of various emulsion and cement contents on an emulsion-treated ferricrete from the HVS Test Section on Road P243/1*, Draft Contract Report CR-2001/77, Transportek, CSIR, Pretoria.

Long FM and Theyse HL, 2001, *Laboratory testing for the HVS Sections on Road P243/1*, Contract Report CR-2001/32, Transportek, CSIR, Pretoria.

Mancotywa WS, 2001, F*irst level analysis report: 2nd Phase HVS testing of the emulsion-treated gravel and foam treated gravel base sections on road P243/1 near Vereeniging*, Draft Contract Report CR-2001/053, Transportek, CSIR, Pretoria.

Steyn WvdM, 2001, *Level one data analysis of HVS tests on foam treated gravel and emulsion-treated gravel on road P243/1: 80 kN and 100 kN test sections*, Contract Report CR-2001/5, Transportek, CSIR, Pretoria.

Theyse HL, 1996, *Overview of the South African Mechanistic Pavement Design Method*, Divisional Publication DP-96/005, Transportek, Pretoria.

Theyse HL, 2000, L*aboratory design models for materials suited to labour intensive construction: Volume I: Report*, Contract Report CR-99/038, Transportek, CSIR, Pretoria.

Wolff H, 1992, *The elasto-plastic behaviour of granular pavement layers in South Africa*, PhD thesis, University of Pretoria, Pretoria.

World Highways, April 2001.

PERFORMANCE MODELS FOR AN EMULSION-TREATED MATERIAL UNDER ACCELERATED PAVEMENT TESTING

J J E LIEBENBERG[1] and A T VISSER[2]

[1]Stewart Scott (Pty) Ltd, P O Box 784506, Sandton, 2146
[2] Department of Civil Engineering, University of Pretoria, Pretoria, 0002

Name	**Johannes Jacobus Erasmus LIEBENBERG**
Profession	Civil Engineer
Years with Firm	2
Years of Experience	5,5
Nationality	South African
Date of Birth	26/01/1972
Key Qualifications	Jaco Liebenberg has been involved in a number of road rehabilitation projects, including the roads between Windhoek and Aris in Namibia, Jwaneng and Sekoma in Botswana, Ficksburg and Clocolan, a number of gravel roads and the rehabilitation design of the main runway at Johannesburg International Airport. Experience includes investigation, design and execution of rehabilitation projects. He has extensive experience in the maintenance of road infrastructure that includes the programming of maintenance activities, maintenance standards, preventative, corrective and emergency maintenance as well as budgeting and planning.
	Jaco provided input at the COLTO road materials- and COLTO Pavement management systems committees. He was also involved in the running of the Free State Pavement Management system and initiated the implementation of a Maintenance Management system. He has experience in the PASCAL and DELPHI computer languages as well as limited programming in C++ within the UNIX/LINUX environment. He has attended a course on the World Bank HDM-4 software package and is able to evaluate the economic feasibility of road projects with this package. Jaco has served as a mentor for emerging contractors, providing support on management, planning and contractual issues.
Professional Registration	**Engineer in Training,** No. 965228
Membership	**South African Institute for Civil Engineering, SAICE** - Member
Education	**Matric**
	Technical High School Louis Botha, 1990
Qualifications	**BEng (Civil)**
	University of Pretoria, 1995
	BEng (Hons) (Transportation)
	University of Pretoria, 1998
Professional History	
04/2000 - Date	**Stewart Scott**
	Engineer
06/1999 - 03/2000	**Milcorp Construction Management**
	Project Manager
01/1996 - 05/1999	**Free State Department of Public Works, Roads and Transport**
	Regional Roads Engineer